INSTITUT DE FRANCE
Académie des sciences

Comptes Rendus

Géoscience

Sciences de la Planète

Ikumi Asano, Nodoka Harada, Atsushi Nakao, Olivier Evrard and Junta Yanai

Impact of radiocesium contamination in flood sediment deposited after the 2019 typhoon on decontaminated fields of Fukushima Prefecture, Japan

Volume 354 (2022), p. 131-140

Published online: 31 March 2022

https://doi.org/10.5802/crgeos.122

Les Comptes Rendus. Géoscience — Sciences de la Planète *sont membres du Centre Mersenne pour l'édition scientifique ouverte*
www.centre-mersenne.org
e-ISSN : 1778-7025

Comptes Rendus
Géoscience — Sciences de la Planète
2022, 354, p. 131-140
https://doi.org/10.5802/crgeos.122

Original Article — External Geophysics, Climate

Impact of radiocesium contamination in flood sediment deposited after the 2019 typhoon on decontaminated fields of Fukushima Prefecture, Japan

Ikumi Asano *,#, [a], **Nodoka Harada**#, [a], **Atsushi Nakao** [a], **Olivier Evrard** [b] **and Junta Yanai** [a]

[a] Graduate School of Life and Environmental Sciences, Kyoto Prefectural University, Kyoto, Japan

[b] Laboratoire des Sciences du Climat et de l'Environnement (LSCE/IPSL), Unité Mixte de Recherche 8212 (CEA/CNRS/UVSQ), Université Paris-Saclay, Gif-sur-Yvette, France

E-mails: ai.asano.ikumi@gmail.com (I. Asano), s821631036@kpu.ac.jp (N. Harada), na_4_ka_triplochiton@kpu.ac.jp (A. Nakao), Olivier.Evrard@lsce.ipsl.fr (O. Evrard), yanai@kpu.ac.jp (J. Yanai)

Abstract. Sediment that has deposited after the flood generated by the 2019 typhoon (referred to as Flood Sediment, FS) was collected along two rivers in eastern Fukushima Prefecture, Japan to determine the total and exchangeable radiocesium (^{137}Cs), and acid-extractable potassium (K) contents. Then, these FS parameters were compared with those of decontaminated soils (DS) in nearby agricultural fields to discuss the potential transfer risk of ^{137}Cs from rivers to nearby remediated soils. While FS had about four times higher total ^{137}Cs content, it showed a three-times lower exchangeable ^{137}Cs content than DS. Furthermore, acid-extractable K referred to as non-exchangeable K (Nex-K) content was high enough to restrict ^{137}Cs transfer from soil to crops for both FS and DS. From these comparisons, we concluded that deposition of FS onto DS may not increase the transfer of ^{137}Cs from soil to crops.

Keywords. Radiocesium, Flood sediment, Decontaminated field, Fukushima, Cesium-137 (^{137}Cs).

Manuscript received 27th November 2021, revised 28th February 2022 and 14th March 2022, accepted 14th March 2022.

1. Introduction

After the accident that occurred at the Fukushima Daiichi Nuclear Power Plant (FDNPP) in March 2011, the Japanese government delineated a Special Decontamination Zone (SDZ) in the areas located within a 20 km radius of the FDNPP or in those areas where the cumulative dose 1 year after the accident was expected to exceed 20 mSv·yr^{-1}. In most of SDZ except for the difficult-to-return-zone corresponding to the most severely contaminated

* Corresponding author.

# Contributed equally.

land located in the close vicinity of FDNPP, topsoil (0–5 cm) was removed from 50% of agricultural land. This soil was taken where ^{137}Cs concentrations exceeded 5000 Bq·kg^{-1} and where it was replaced with a 5 cm layer of "clean" material often corresponding to mountainous sand [Evrard et al., 2019]. Then, the coarse material showing a sandy texture was thoroughly mixed with residual soils in depth to prepare the soil for restarting cultivation by the returnees. These decontamination activities decreased the ^{137}Cs concentrations in topsoil by about 80% compared to the original levels [Kurokawa et al., 2019]. In contrast, decontaminated forested areas within the SDZ was restricted to those zones lying within 20 m around residential areas and along roads [Ministry of the Environment, 2013].

In October 2019, Typhoon Hagibis stuck the eastern part of Fukushima Prefecture and generated the widespread overflow of the rivers flowing across the SDZ. Sediment transported by the typhoon-generated flooding, which was referred to as flood sediment (FS), got deposited in the decontaminated agricultural fields at many locations along the rivers. Evrard et al. [2020] estimated that approximately 40% of the sediment deposited during the flood induced by the Hagibis typhoon originated from forested areas. Since most of the forest soils in the SDZ were virtually not decontaminated and maintained high levels of ^{137}Cs concentrations [Onda et al., 2020], the deposition of sediment following the typhoon-induced flooding of decontaminated fields along the river network may increase the transfer potential of ^{137}Cs from soil to crops in these decontaminated agricultural fields. However, to the best of our knowledge, neither the mobility of ^{137}Cs found on FS nor the transfer potential of ^{137}Cs to the crops in these previously decontaminated fields has been investigated so far.

Therefore, this study investigated total and exchangeable radiocesium (^{137}Cs) content, and acid-extractable potassium (AE-K) contents for FS and DS in agricultural fields in the SDZ to discuss the impact of FS deposition on the potential migration of ^{137}Cs from decontaminated agricultural land to crops. The AE-K, which is generally referred to as Nex-K in soil science, provides a good indicator to predict the inhibitory effect of K on ^{137}Cs uptake by plants. Kurokawa et al. [2020] determined that the soils with Nex-K > 50 mg K_2O 100 g^{-1} showed sufficiently low soil-to-rice transfer risk of ^{137}Cs in Fukushima.

2. Materials and methods

2.1. *Sampling sites and sampling preparation of flood sediments and decontaminated soils*

FS and DS samples were collected along Niida River and Mano River within Iitate Village, Fukushima, Japan, which is located about 40 km northwest from the FDNPP. These rivers overflowed at many locations following Typhoon Hagibis (typhoon 19) in October 2019. Their catchments include upstream mountainous plateaus at an altitude of 700–900 m above sea level connected to a flat coastal plain by deep and strongly incised rivers [Chartin et al., 2017]. About two-thirds of the land in these catchments is occupied by forested areas. Most of the agricultural fields along these rivers were used as paddy fields before the 2011 nuclear accident. Geologically, granite and granodiorite are dominant in the area, with a minor occurrence of sedimentary rocks and basalts [Geological Survey of Japan, AIST, 2022].

DS samples were collected using a shovel from the upper 0–15 cm layer of surface soil from 18 decontaminated fields in March 2019. In each field, subsamples of soil were collected from five points (at the center and the four vertices of a square with a side length of 15 m) and mixed together well. Also, FS samples were collected from 19 points where river flooding occurred in the close vicinity of the DS sampling sites after the Hagibis typhoon in October 2019 (Figure 1). The FS samples correspond to fresh sediments deposited as a fine material draped on the upper part of the embankment along the Mano River ($n = 6$) and Niida River ($n = 13$). FS samples were collected from the uppermost layer of about 0–1 cm of fresh sediments using a shovel. The DS and FS samples were dried at room temperature and sieved to <2.0 mm.

2.2. *Radiocesium analyses*

Total and exchangeable ^{137}Cs contents in FS or DS were determined following the method of Kurokawa et al. [2019]. Approximately 20–40 g of the soil sample was filled in a polyethylene vial (20 cm^3). The vial

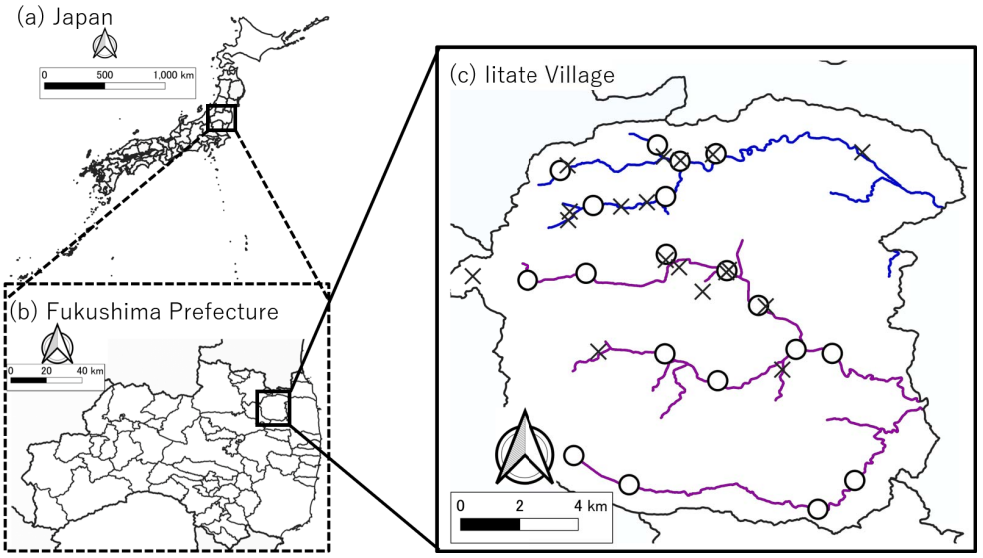

Figure 1. Location of sampling sites of Decontaminated Soils—DS (×) and Flood Sediment—FS (○) in the vicinity of Mano (blue) and Niida (purple) Rivers, Fukushima Prefecture, Japan.

was set in an auto gamma counter with a NaI (Tl) detector (2480WIZARD2, PerkinElmer, Waltham, Massachusetts, USA, Radioisotope Research Center of Kyoto Prefectural University) to determine the gamma activity (between 589 and 735 keV). To determine the exchangeable ^{137}Cs content, duplicates of 50 g of sample were shaken with 250 mL of 1 mol·L^{-1} ammonium acetate (CH_3COONH_4) for 24 h at 20 °C. The extracts were heated on a hot plate and concentrated to about 20 mL. The concentrated solution was measured with NaI (TI) detector in the same way as for total ^{137}Cs content. The data were calibrated by comparing the measured values with those obtained using a Ge semiconductor detector connected to a multichannel analyzer system (GC-4018, Canberra, Japan, Radioisotope Research Center of Fukushima University). Details of this procedure are provided by Kurokawa et al. [2019].

The ^{137}Cs exchangeable fraction (%), i.e., the percentage of exchangeable ^{137}Cs content compared to the total ^{137}Cs content, was calculated using the following equation:

[^{137}Cs exchangeable fraction (%)] = [Exchangeable ^{137}Cs content in FS and DS (Bq·kg^{-1})]/[Total ^{137}Cs content in FS and DS (Bq·kg^{-1})] × 100.

2.3. *Particle size distribution*

Particle size distribution, i.e., respective content in coarse sand (2000–200 μm), fine sand (200–50 μm), and silt and clay (< 50 μm) in FS and DS, was assessed by pipetting and sieving after removing soil organic matter with oxidizing reagents.

2.4. *Total carbon content*

The total carbon (TC) content in sample was measured, as an indicator of total organic matter content, determined by the dry combustion method with an NC analyzer (NC-95A, Smika Chem. Anal. Service, Tokyo, Japan) and gas chromatography (GC-8A, Shimadzu, Kyoto, Japan) after fine grinding with agate mortar.

2.5. *X-ray diffraction (XRD) analysis*

XRD diffractogram was determined using the matrix flushing technique [Chung, 1974]. 1.0-g soil sample was mixed with 7-mL methanol and 0.25-g α-Al_2O_3 (Baikalox 3.0CR, Bakowski, France) as internal standard and finely-ground to a powder using

a grinding machine (XRD-Mill Mcrone, Retsch, German) for 10 min. The mixed powder was packed into a holder to ensure a random sample orientation and then irradiated from 5° to 65° two-theta using CuKα-radiation, with 0.02° steps and a counting rate of 10° per min by XRD (MiliFlex 600, Rigaku, Tokyo, Japan). The diffraction peak at 8.8° two-theta corresponded to the 1.0 nm lattice spacing associated with the presence of non-expanding mica layers [Kitayama et al., 2020, Ogasawara et al., 2019]. As K in these non-expanding layers is the primary source of Nex-K, XRD_{micas} provided a rough index of the amount of Nex-K present. Therefore, XRD_{micas} was calculated by the following equation:

$$[XRD_{micas}] = [\text{Intensity of 1.0 nm (cps)}]/[\text{Intensity of 0.25 nm (cps)}],$$

where the intensity of 1.0 and 0.25 nm are the measured intensities of the (001) reflections derived from mica and (104) reflections derived from α-Al_2O_3, respectively.

2.6. *Non-exchangeable K as an indicator of acid-extractable K*

Nex-K could be used as a good proxy of K phytoavailable fraction especially in mica-rich soil [Mengel and Rahmatullah, 1994, Surapaneni et al., 2002]. Kurokawa et al. [2020] and Wakabayashi et al. [2022] reported that the Nex-K reduced RCs crop migration as well as that of exchangeable K (Ex-K). The Nex-K content of the FS and DS samples was determined by subtracting Ex-K from the estimation of K concentration determined as the elemental content extracted with the hot nitric acid method [Helmke and Sparks, 1996]. The Nex-K is often used as an indicator of the phytoavailable K fraction, which is not extractable with ion-exchange reaction. A 2.50-g soil sample was gently heated using a hot plate (EA-DC10, ZOJIRUSHI, Osaka, Japan) at nearly 100 °C for 15 min with 25.0 mL of 1 mol·L^{-1} HNO_3 after boiling started. After cooling, the extract was filtered and filled up to 100 mL with 0.1 mol·L^{-1} HNO_3. The K content of the extract solution was determined via Atomic Absorption Spectroscopy (AAS) (AA -6200, Shimadzu, Kyoto, Japan). To determine the Ex-K content, the DS and FS samples were shaken with 1 mol·L^{-1} CH_3COONH_4 at pH 7.0 in a soil:solution ratio of 1:5 for 30 min at 20 °C. The suspension was centrifuged, and the supernatant was collected by filtration. These processes were repeated three times. Approximately 75 mL of supernatant was brought up to a total volume of 100 mL with 1 mol·L^{-1} CH_3COONH_4, and the K content of this solution was determined using the same instruments.

3. Results and discussion

3.1. *Total ^{137}Cs content in flood sediment and its controlling factors*

The total ^{137}Cs content in FS reached on average 4.2 kBq·kg^{-1} (Table 1). This observed value was lower than that obtained in FS collected along the same two rivers in 2011 and 2015 [Chartin et al., 2017]. Previous research indicated that the amount of ^{137}Cs had strongly decreased in river sediment and in the soil surface in 2019 compared to 2011 [Evrard et al., 2021, Funaki et al., 2019, Iwagami et al., 2017, Yoshimura et al., 2016], which further supports the results obtained in the current study.

Typhoon Hagibis caused debris flows that apparently excavated soils from contaminated topsoil layers, and much less contaminated subsurface soils as shown for FS in Miyagi Prefecture [Moriguchi et al., 2021]. Highly contaminated surface soils from forested areas were therefore likely mixed with subsurface soils from landslides and channel bank collapse events, which may consequently explain the overall low total ^{137}Cs content in FS.

Although total ^{137}Cs contents in FS reached an average value of 4.2 kBq·kg^{-1}, they showed a wide range of values varying from 0.51 to 16 kBq·kg^{-1} (Table 1). Potential explanation factors relating to this variation were investigated by means of the Pearson correlation analysis, which revealed that the silt + clay content of FS, averaging 18% (range: 4.9 to 36%), was positively correlated with total ^{137}Cs content ($r = 0.59, p < 0.01$) (Figure 2a). This may reflect the strong interaction of ^{137}Cs with sediments, i.e., the finer mineral particles have a larger specific surface area and a higher proportion of 2:1 clay minerals, which can strongly adsorb Cs in their frayed-edge sites [Fan et al., 2014, He and Walling, 1996, Nakao et al., 2012].

Organically-bound ^{137}Cs was not considered as a major fraction of the total ^{137}Cs in FS. We observed few macro-organic material (e.g., leaves and litter from forest vegetation) in the field affected by

Table 1. Selected physicochemical properties of FS

FS sample	Total ^{137}Cs, Bq·kg^{-1}	Exchangeable ^{137}Cs, Bq·kg^{-1}	^{137}Cs exchangeable fraction, %	Coarse sand	Fine sand	Silt + clay	PIRmica	Ex-K	Nex-K	TC, g·kg^{-1}
				%				mg K_2O 100 g^{-1}		
1	15,508	292	1.9	43	21	36	1.0	28	126	4.0
2	1038	N.D	N.D	71	20	9.0	1.0	22	157	N.D
3	1355	N.D	N.D	75	14	11	1.3	19	153	N.D
4	N.D	N.D	N.D	44	24	32	1.0	15	163	N.D
5	5268	189	3.6	37	31	32	0.62	28	201	4.6
6	5647	188	3.3	58	18	24	0.87	16	110	4.5
7	676	N.D	N.D	92	4.5	3.9	1.0	10	99	N.D
8	5170	210	4.1	73	10	17	0.44	28	80	5.0
9	705	N.D	N.D	77	13	11	0.80	12	93	N.D
10	778	N.D	N.D	86	7.2	7.2	1.1	9	148	N.D
11	2188	70	3.2	52	17	30	1.7	19	317	2.6
12	1273	N.D	N.D	38	30	33	0.66	34	98	N.D
13	513	N.D	N.D	66	22	12	0.86	10	136	N.D
14	4430	N.D	N.D	49	28	23	1.4	57	172	N.D
15	16,374	352	2.2	58	15	27	1.1	26	163	8.1
16	3965	165	3.2	71	17	12	1.3	12	173	1.4
17	776	N.D	N.D	68	20	12	1.6	25	282	N.D
18	9360	428	4.6	73	11	17	1.0	34	168	2.3
19	3164	210	6.6	56	32	12	1.3	11	223	0.47
20	1560	N.D	N.D	71	21	7.9	1.0	12	173	N.D
Median	4197	234	3.6	63	19	18	1.0	21	162	3.7
Max	16,374	428	6.6	92	32	36	1.7	57	317	8.1
Min	513	70	1.9	37	4.5	3.9	0.44	9.5	80	0.47

FS migration via flooding events. Since DS fields were not cultivated at that time, crops could not have trapped macro-organic material, which would instead have been carried away by the river water. As previously reported, ^{137}Cs in soils and sediments was found to be bound predominantly to the soil mineral phase whereas it was found bound to a lesser extent to organic matter [Koarashi et al., 2019, Tsukada et al., 2008]. The amount of total carbon in the FS was low, with an average of 3.7 g·kg^{-1} (range: 0.47 to 8.1 g·kg^{-1}), and it was found not to be significantly correlated with total ^{137}Cs content or the ^{137}Cs exchangeable fraction (Figure 2b). Based on these results we considered that the amount of organic matter-bound ^{137}Cs in the FS should only provide a minor contribution, if any, to the total ^{137}Cs content.

3.2. *Comparing total* ^{137}Cs *content and* ^{137}Cs *exchangeable fraction between FS and DS*

The total ^{137}Cs content in DS reached on average 1.2 ± 2.0 kBq·kg^{-1} (Figure 3). The entire range of values (Table 2) was less than one-fifth of the total ^{137}Cs content in agricultural land observed before decontamination in Iitate Village [Ministry of Agriculture, F. and F., 2011]. A drastic decrease in total ^{137}Cs content after decontamination was observed in the agricultural fields in Tomioka Town [Kurokawa et al., 2019]. Thus, decontamination activities for agricultural fields in Iitate village were thus confirmed to have effectively reduced the total ^{137}Cs content in surface soils corresponding to about 80% in a decrease of the initial contamination levels. Although total ^{137}Cs was not significantly different between FS

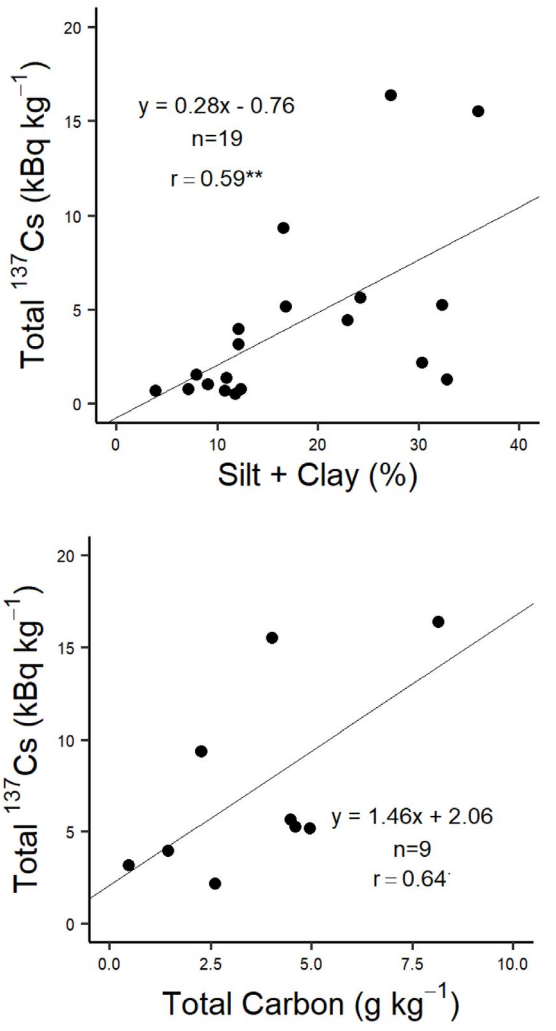

Figure 2. Relationship between total ^{137}Cs content and silt + clay content of FS (a) and total ^{137}Cs content of FS and total carbon content of FS (b). Unpaired t-test, **: $p < 0.01$, ': $p < 0.1$.

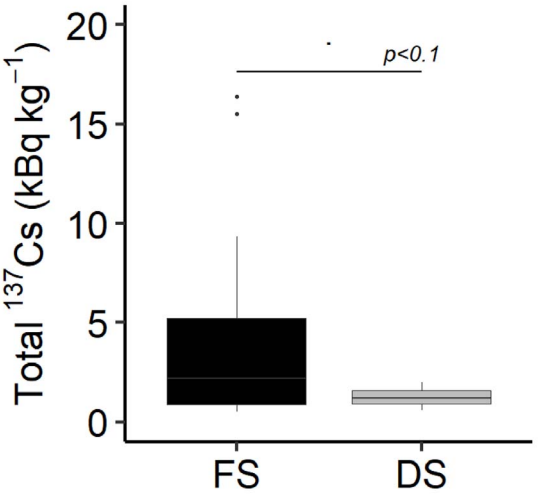

Figure 3. Box plots showing total ^{137}Cs content of FS and DS. Each box-and-whisker shows five-number summary of a set of data: minimum, lower quartile, median, upper quartile, and maximum, whereas filled circles show outliers. Unpaired t-test, *: $p < 0.1$.

and DS, this value range was lower than that of FS (Figure 3). These comparisons suggest that FS deposition on DS may lead to a new increase in their total ^{137}Cs content, at least in their surface layer. However, the increase in total ^{137}Cs content due to FS deposition, if any, may not raise the transfer risk of ^{137}Cs from soil to crops for the following reasons. First, our field observations in Iitate Village confirmed that the thickness of the FS layer deposited on decontaminated fields following the flooding reached at most about 1 cm in depth. Assuming that the thin FS layer contained a total ^{137}Cs activity of 4.2 kBq·kg^{-1} mixed with 15 cm of the plowed layer with a total ^{137}Cs content of 1.2 kBq·kg^{-1}, the total ^{137}Cs content of the entire profile would only increase by 15% to an average of about 1.4 kBq·kg^{-1}. While this is a rough estimation based on field observation of the thickness of sediments deposited in several agricultural fields, it indicates that the FS incorporation into a realistic larger volume of soil will not lead to a strong increase in the total ^{137}Cs content in decontaminated fields. It should be emphasized that the 1 cm thickness was an exceptional case for FS migration to DS. The average trend was unfortunately not quantitatively recorded in this study, but more accurate observation is needed in the future when larger volumes are involved. A comprehensive risk assessment would require a more detailed calculation of the thickness of sediment deposited onto agricultural soils.

Second, the average ^{137}Cs exchangeable fraction of FS was 3.7%, only about one-third of that rate obtained from DS (i.e., 9.8%) (Figure 4). Whereas the ^{137}Cs exchangeable fraction from DS remained in the medium range of values (range: 6.5 to 16%) previously reported for ^{137}Cs contaminated soils in

Table 2. Selected physicochemical properties of DS

DS sample	Total ^{137}Cs, Bq·kg^{-1}	Exchangeable ^{137}Cs, Bq·kg^{-1}	^{137}Cs exchangeable fraction, %	Coarse sand	Fine sand	Silt + clay	PIRmica	Ex-K	Nex-K	TC, g·kg^{-1}
				%				mg K_2O 100 g^{-1}		
1	733	106	14.5	21	21	57	0.03	48	48	1.7
2	913	70	7.6	51	12	37	2.4	41	203	1.0
3	937	80	8.6	39	24	37	0.84	34	125	1.4
4	1176	193	16.4	36	18	47	0.05	30	14	2.3
5	N.D	N.D	N.D	35	19	46	0.51	22	130	2.4
6	N.D	N.D	N.D	51	20	29	1.5	11	202	0.24
7	N.D	N.D	N.D	35	30	36	1.1	14	269	1.1
8	1407	92	6.5	37	30	33	2.2	9	364	0.88
9	N.D	N.D	N.D	27	28	45	0.89	17	275	0.57
10	N.D	N.D	N.D	30	29	41	1.5	16	405	0.47
11	N.D	N.D	N.D	44	29	27	3.0	11	461	0.41
12	1673	168	10.0	33	24	43	0.23	13	137	1.0
13	N.D	N.D	N.D	36	34	30	2.8	23	396	0.60
14	1683	126	7.5	34	35	31	2.0	11	257	1.2
15	1272	83	6.6	29	28	43	1.2	21	185	1.8
16	N.D	N.D	N.D	34	24	42	0.29	29	107	1.1
17	626	61	9.8	39	29	31	1.4	12	293	1.1
18	1982	208	10.5	22	28	50	0.13	38	56	1.8
Median	1240	119	10	35	26	39	1.2	22	218	1.2
Max	1982	208	16	51	35	57	3.0	48	461	2.4
Min	626	61	6.5	21	12	27	0.03	9.3	14	0.24

Fukushima, corresponding values from FS remained close to the lowest values previously reported for contaminated soils and sediments [Kurokawa et al., 2019, Ogasawara et al., 2019, Saito et al., 2014]. These data suggested that ^{137}Cs was assumed not to be desorbed easily from FS particles. Third, FS showed high levels of Nex-K content, with an average of 162 mg K_2O 100 g^{-1} (range: 80 to 317 mg K_2O 100 g^{-1}), as high as in DS (i.e., on average 218 mg K_2O 100 g^{-1}). Most of these values were higher than the recommended value (i.e., 50 mg K_2O 100 g^{-1}), above which the transfer rate of ^{137}Cs from soil to crops was confirmed to be low [Kurokawa et al., 2020]. Since ^{137}Cs exchangeable fraction and Nex-K content in soil control soil-to-plant transfer of ^{137}Cs rather than the total ^{137}Cs content itself, these results may overall lead to the conclusion that FS deposition in decontaminated fields may not increase the transfer risk of ^{137}Cs in the case of Iitate Village in Fukushima.

A missing source of ^{137}Cs that might have been incorporated into the DS field was dissolved ^{137}Cs in flood water. Takata et al. [2020] indeed showed higher dissolved ^{137}Cs activity in nearshore water after the 2019 typhoon. Although we could not measure the amount of ^{137}Cs in DS after the typhoon, it is unlikely that dissolved ^{137}Cs may be supplied to DS after the deposition of FS, as the ^{137}Cs exchangeable fraction was found to be lower than 5% in the current research.

3.3. *Factors relating to Nex-K content of FS and DS*

The Nex-K content of FS and DS (i.e., on average 162 and 218 mg K_2O 100 g^{-1}) was relatively high, compared to those levels previously found in other areas of Fukushima Prefecture, including a mean value of 66 mg K_2O 100 g^{-1}, obtained on 173 farmland soils in Tomioka Town [Kurokawa et al., 2019]. The regional

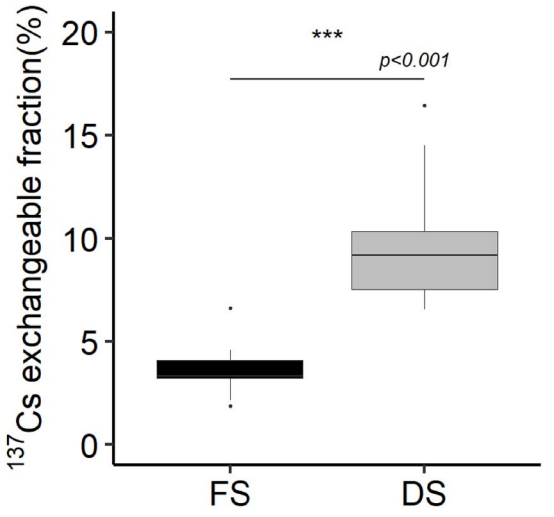

Figure 4. Box plots showing the ^{137}Cs exchangeable fraction of FS and DS. Each box-and-whisker shows five-number summary of a set of data: minimum, lower quartile, median, upper quartile, and maximum, whereas filled circles show outliers. Unpaired t-test, ***: $p < 0.001$.

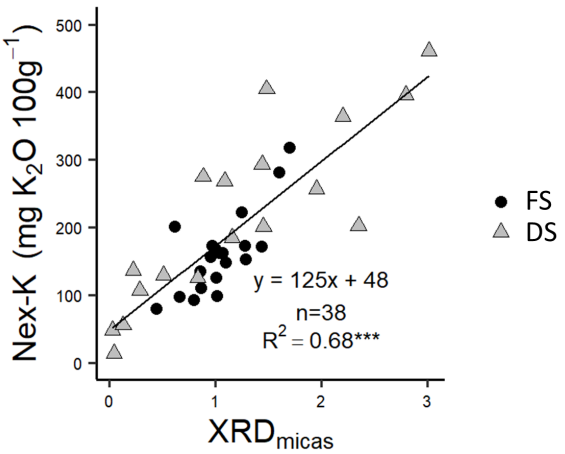

Figure 5. Relationship between XRD$_{micas}$ and Nex-K of FS and DS.

difference in Nex-K content may reflect to a large extent the type of base rock in each area. For example, Iitate Village is a locality surrounded by Abukuma granite mountains. Therefore, the fluvisols on which cropland was installed in the valleys, and the coarse material extracted from the quarries to replace the contaminated upper soil layer during remediation, both contain minerals, derived from granite or granitoid, which in turn contains biotite as a major rock-forming mineral. To investigate whether the quantity of mica defines Nex-K, we investigated the correlation between Nex-K and XRD$_{micas}$, which is an index of mica quantity, and found that Nex-K showed significantly positive correlation with XRD$_{micas}$ ($p < 0.001$) (Figure 5). This strongly supports the hypothesis that Nex-K content was primarily controlled by micaceous minerals probably derived from granite. Granite and granodiorite widely cover the surfaces of Abukuma Highlands, which have been weathered to supply biotite to watershed areas via river water transfer. Several studies on the mineral composition of sediments have indicated the occurrence of biotite in this material [Fan et al., 2014, Konoplev et al., 2021]. Accordingly, the K release potential of FS which was found to be comparable to that of DS should be probably ubiquitous across this region. The granitic biotite in both FS and DS may contribute to long-term K resources for plants, which effectively inhibit ^{137}Cs migration from soil to crops.

4. Conclusions

Total ^{137}Cs content in FS along Mano and Niida Rivers caused by Typhoon Hagibis in October 2019 was about four times larger than that found in decontaminated agricultural soils in Iitate Village. However, the ^{137}Cs exchangeable fraction of FS was low and the Nex-K content was as high as that of DS, suggesting a low potential risk of the FS to transfer ^{137}Cs from soil to plant. In the future, it will be important to elucidate in detail the behavior and K supply capacity of RCs in the forest area, which is the origin of FS.

Conflicts of interest

Authors have no conflict of interest to declare.

Acknowledgments

We would like to thank Dr. Yuzo Mampuku (Institute for Agro-Environmental Sciences, NARO) and inhabitants from Iitate Village for helping collect the soil samples, and Dr. Kenta Ikazaki (Japan International Research Center for Agricultural Sciences) for his

kind assistance in the GIS analysis. We thank the Radioisotope Research Center of Kyoto Prefectural University, where we undertook our ^{137}Cs experiments. We also thank the anonymous reviewers and the editor for their constructive comments, which helped to improve this manuscript. The fieldwork of the French partner was funded by the AMORAD (ANR-11-RSNR-0002) project, under the supervision of the French National Research Agency (ANR, Agence Nationale de la Recherche). The fieldwork and in vitro experiments were mainly funded by JSPS bilateral program (No. 1082680). The support of CNRS (Centre National de la Recherche Scientifique, France) and JSPS (Japan Society for the Promotion of Science) through the funding of collaboration projects (grant no. PRC CNRS JSPS 2019-2020, no.10; CNRS International Research Project–IRP–MITATE Lab) is also gratefully acknowledged.

References

Chartin, C., Evrard, O., Laceby, J. P., Onda, Y., Ottlé, C., Lefèvre, I., and Cerdan, O. (2017). The impact of typhoons on sediment connectivity: lessons learnt from contaminated coastal catchments of the Fukushima Prefecture (Japan). *Earth Surf. Process. Landf.*, 42(2), 306–317.

Chung, F. H. (1974). Quantitative interpretation of x-ray diffraction patterns of mixtures. I. matrix-flushing method for quantitative multicomponent analysis. *J. Appl. Cryst.*, 7, 519–525.

Evrard, O., Chartin, C., Laceby, J. P., Onda, Y., Wakiyama, Y., Nakao, A., Cerdan, O., Lepage, H., Jaegler, H., Vandromme, R., Lefèvre, I., and Bonté, P. (2021). Radionuclide contamination in flood sediment deposits in the coastal rivers draining the main radioactive pollution plume of Fukushima Prefecture, Japan (2011–2020). *Earth Syst. Sci. Data*, 13(6), 2555–2560.

Evrard, O., Durand, R., Nakao, A., Laceby, J. P., Lefèvre, I., Wakiyama, Y., Hayashi, S., Asanuma-Brice, C., and Cerdan, O. (2020). Impact of the 2019 typhoons on sediment source contributions and radiocesium concentrations in rivers draining the Fukushima radioactive plume, Japan. *C. R. Geosci.*, 352(3), 199–211.

Evrard, O., Laceby, J. P., and Nakao, A. (2019). Effectiveness of landscape decontamination following the fukushima nuclear accident: A review. *SOIL*, 5(2), 333–350.

Fan, Q., Tanaka, K., Sakaguchi, A., Kondo, H., Watanabe, N., and Takahashi, Y. (2014). Factors controlling radiocesium distribution in river sediments: Field and laboratory studies after the Fukushima Dai-ichi Nuclear Power Plant accident. *Appl. Geochem.*, 48, 93–103.

Funaki, H., Yoshimura, K., Sakuma, K., Iri, S., and Oda, Y. (2019). Evaluation of particulate ^{137}Cs discharge from a mountainous forested catchment using reservoir sediments and sinking particles. *J. Environ. Radioact.*, 210, article no. 105814.

Geological Survey of Japan, AIST (2022). Seamless digital geological map of Japan 1: 200,000. February 14, 2022 version. Geological Survey of Japan, National Institute of Advanced Industrial Science and Technology.

He, Q. and Walling, D. E. (1996). Interpreting particle size effects in the adsorption of ^{137}Cs and unsupported ^{210}Pb by mineral soils and sediments. *J. Environ. Radioact.*, 30(2), 117–137.

Helmke, P. A. and Sparks, D. L. (1996). Lithium, sodium, potassium, rubidium, and cesium. In *Methods of Soil Analysis: Part 3. Chemical Methods*, SSSA Book Series no. 5, pages 559–562. Soil Science Society of America, Inc., Madison, WI.

Iwagami, S., Tsujimura, M., Onda, Y., Nishino, M., Konuma, R., Abe, Y., Hada, M., Pun, I., Sakaguchi, A., Kondo, H., Yamamoto, M., Miyata, Y., and Igarashi, Y. (2017). Temporal changes in dissolved ^{137}Cs concentrations in groundwater and stream water in Fukushima after the Fukushima Dai-ichi Nuclear Power Plant accident. *J. Environ. Radioact.*, 166, 458–465.

Kitayama, R., Yanai, J., and Nakao, A. (2020). Ability of micaceous minerals to adsorb and desorb caesium ions: Effects of mineral type and degree of weathering. *Eur. J. Soil Sci.*, 71(4), 641–653.

Koarashi, J., Nishimura, S., Atarashi-Andoh, M., Muto, K., and Matsunaga, T. (2019). A new perspective on the ^{137}Cs retention mechanism in surface soils during the early stage after the Fukushima nuclear accident. *Sci. Rep.*, 9(1), article no. 7034.

Konoplev, A., Wakiyama, Y., Wada, T., Udy, C., Kanivets, V., Ivanov, M. M., Komissarov, M., Takase, T., Goto, A., and Nanba, K. (2021). Radiocesium distribution and mid-term dynamics in the ponds of the Fukushima Dai-ichi nuclear power plant exclu-

sion zone in 2015–2019. *Chemosphere*, 265, article no. 129058.

Kurokawa, K., Nakao, A., Tsukada, H., Mampuku, Y., and Yanai, J. (2019). Exchangeability of ^{137}Cs and K in soils of agricultural fields after decontamination in the eastern coastal area of Fukushima. *Soil Sci. Plant Nutr.*, 65(4), 401–408.

Kurokawa, K., Nakao, A., Wakabayashi, S., Fujimura, S., Eguchi, T., Matsunami, H., and Yanai, J. (2020). Advanced approach for screening soil with a low radiocesium transfer to brown rice in Fukushima based on exchangeable and nonexchangeable potassium. *Sci. Total Environ.*, 743, article no. 140458.

Mengel, K. and Rahmatullah (1994). Exploitation of potassium by various crop species from primary minerals in soils rich in micas. *Biol. Fert. Soils*, 17, 75–79.

Ministry of Agriculture, F. and F. (2011). Analytical value of radioactive cesium in agricultural land soil. https://www.affrc.maff.go.jp/docs/press/pdf/110830-24.pdf. (Latest access on 26 February 2022).

Ministry of the Environment (2013). *Decontamination-Related Guidelines.* 2nd edition, http://josen.env.go.jp/material/pdf/josen-gl-full_ver2_supplement_1803.pdf. (Latest access on 26 February 2022).

Moriguchi, S., Matsugi, H., Ochiai, T., Yoshikawa, S., Inagaki, H., Ueno, S., Suzuki, M., Tobita, Y., Chida, T., Takahashi, K., Shibayama, A., Hashimoto, M., Kyoya, T., and Dolojan, N. L. J. (2021). Survey report on damage caused by 2019 Typhoon hagibis in Marumori town, Miyagi prefecture, Japan. *Soils Found.*, 61(2), 586–599.

Nakao, A., Funakawa, S., Takeda, A., Tsukada, H., and Kosaki, T. (2012). The distribution coefficient for cesium in different clay fractions in soils developed from granite and paleozoic shales in japan. *Soil Sci. Plant Nutr.*, 58(4), 397–403.

Ogasawara, S., Eguchi, T., Nakao, A., Fujimura, S., Takahashi, Y., Matsunami, H., Tsukada, H., Yanai, J., and Shinano, T. (2019). Phytoavailability of ^{137}Cs and stable Cs in soils from different parent materials in Fukushima, Japan. *J. Environ. Radioact.*, 198, 117–125.

Onda, Y., Taniguchi, K., Yoshimura, K., Kato, H., Takahashi, J., Wakiyama, Y., Coppin, F., and Smith, H. (2020). Radionuclides from the Fukushima Daiichi nuclear power plant in terrestrial systems. *Nat. Rev. Earth Environ.*, 1(12), 644–660.

Saito, T., Makino, H., and Tanaka, S. (2014). Geochemical and grain-size distribution of radioactive and stable cesium in Fukushima soils: Implications for their long-term behavior. *J. Environ. Radioact.*, 138, 11–18.

Surapaneni, A., Palmer, A. S., Tillman, R. W., Kirkman, J. H., and Gregg, P. E. H. (2002). The mineralogy and potassium supplying power of some loessial and related soils of New Zealand. *Geoderma*, 110, 191–204.

Takata, H., Aono, T., Aoyama, M., Inoue, M., Kaeriyama, H., Suzuki, S., Tsuruta, T., Wada, T., and Wakiyama, Y. (2020). Suspended particle-water interactions increase dissolved ^{137}Cs activities in the nearshore seawater during typhoon hagibis. *Environ. Sci. Technol.*, 54(17), 10678–10687.

Tsukada, H., Takeda, A., Hisamatsu, S., and Inaba, J. (2008). Concentration and specific activity of fallout ^{137}Cs in extracted and particle-size fractions of cultivated soils. *J. Environ. Radioact.*, 99(6), 875–881.

Wakabayashi, S., Eguchi, T., Nakao, A., Azuma, K., Fujimura, S., Kubo, K., Saito, M., Matsunami, H., and Yanai, J. (2022). Effectiveness of non-exchangeable potassium quantified by mild tetraphenyl-boron extraction in estimating radiocesium transfer to soybean in Fukushima. *Sci. Total Environ.*, 820, article no. 153119.

Yoshimura, K., Onda, Y., and Wakahara, T. (2016). Time dependence of the ^{137}Cs concentration in particles discharged from rice paddies to freshwater bodies after the Fukushima Daiichi NPP accident. *Environ. Sci. Technol.*, 50(8), 4186–4193.